Physica Medica 48 (2018) 47–54

Contents lists available at ScienceDirect

Physica Medica

journal homepage: www.elsevier.com/locate/ejmp

Original paper

Detection of structural abnormalities of cortical and subcortical gray matter in patients with MRI-negative refractory epilepsy using neurite orientation dispersion and density imaging

Masoumeh Rostampour[a], Hassan Hashemi[b,*], Seyed Morteza Najibi[c], Mohammad Ali Oghabian[a]

[a] Department of Medical Physics and Biomedical Engineering, School of Medicine, Tehran University of Medical Sciences, Tehran, Iran
[b] Advanced Diagnostic and Interventional Radiology Research Center (ADIR), Tehran University of Medical Sciences, Tehran, Iran
[c] Department of Statistics, School of Sciences, Shiraz University, Shiraz, Iran

ARTICLE INFO

Keywords:
NODDI
DTI
MRI negative refractory epilepsy
Cortical and subcortical gray matter

ABSTRACT

Purpose: NODDI (Neurite Orientation Dispersion and Density Imaging) and DTI (Diffusion tensor imaging) may be useful in identifying abnormal regions in patients with MRI-negative refractory epilepsy. The aim of this study was to determine whether NODDI and DTI maps including neurite density (ND), orientation dispersion index (ODI), mean diffusivity (MD) and fractional anisotropy (FA) can detect structural abnormalities in cortical and subcortical gray matter (GM) in these patients. The correlation between these parameters and clinical characteristics of the disease was also investigated.

Methods: NODDI and DTI maps of 17 patients were obtained and checked visually. Region of interest (ROI) was drawn on suspected areas and contralateral regions in cortex. Contrast-to-noise ratio (CNR) was determined for each region. Furthermore volumetric data and mean values of ND, ODI, FA and MD of subcortical GM structures were calculated in both of the patients and controls. Finally, the correlations of these parameters in the subcortical with age of onset and duration of epilepsy were investigated.

Results: Cortical abnormalities on ODI images were observed in eight patients qualitatively. CNR of ODI was significantly greater than FA and MD. The subcortical changes including decrease of FA and ND and increase of ODI in left nucleus accumbens and increase of the volume in right amygdala were detected in the patients.

Conclusions: The results revealed that NODDI can improve detection of microstructural changes in cortical and subcortical GM in patients with MRI negative epilepsy.

1. Introduction

About one third of patients with focal epilepsy are intractable to antiepileptic drug treatments [1–4]. Surgery can be an adequate option for treatment of these patients [5]. Detection of the epileptogenic focus is vital to have an appropriate surgical outcomes [6–8]. MRI is a non-invasive technique for presurgical evaluation of epileptic patients, however around 20–30% of these patients have not any obvious lesion on conventional MRI [9]. Approximately, 20–30% of patients with temporal lobe epilepsy and 20–40% of patients with extra temporal lobe epilepsy are included in MRI negative epilepsy [10–12]. Pathological studies have shown that despite heterogeneity of resected surgical specimens, focal cortical dysplasia is the most frequent cause of MRI negative refractory epilepsy [13–18]. The absence of a lesion on MRI leads to failure in surgery of MRI-negative patients [16]. Seizure-free rate after epilepsy surgery in the patients with MRI-lesional is approximately twice of the patients with MRI-negative epilepsy [19].

Detection of lesion in patients previously reported as MRI-negative can modify the planning of presurgical treatment and improve the surgical outcome [20]. In Bein study, re-evaluation of presurgical MRI of nine MRI-negative patients undergoing surgery showed that 8 patients had subtle lesions in the same area of resected tissue. These lesions were not seen because of their small sizes [19]. Therefore in MRI negative patients, it is too difficult to diagnose a lesion and other advanced imaging techniques are required for detecting lesions.

Diffusion tensor imaging (DTI) is an MRI-based neuroimaging technique. DTI indices including fractional anisotropy (FA) and mean diffusivity (MD) are sensitive to tissue microstructure and diffusion changes in the white matter. DTI has been used in characterizing the epileptogenic zone in patients with MRI negative epilepsy [21–23]. A new microstructure imaging method called Neurite Orientation Dispersion and Density Imaging (NODDI) was introduced by Zhang and

* Corresponding author.
E-mail addresses: m-rostampour@razi.tums.ac.ir (M. Rostampour), hashemi_mic@yahoo.com (H. Hashemi), oghabian@tums.ac.ir (M.A. Oghabian).

https://doi.org/10.1016/j.ejmp.2018.03.005
Received 26 December 2017; Received in revised form 3 March 2018; Accepted 6 March 2018

colleagues in 2012 [24]. Unlike the DTI, which assumes each voxel contains a single tissue compartment, the intrinsic assumption in NODDI is that each voxel consists of three compartments including intra-neurite, extra-neurite and cerebrospinal fluid (CSF) [24]. NODDI is used to estimate the microstructure of dendrites and axons in both of the gray and white matter [24]. NODDI indices including neurite density (ND) and orientation dispersion index (ODI) estimate the volume fraction of intracellular and the degree of fiber coherence, respectively [24,25]. As of yet no study has been worked on the use of NODDI parameters in MRI negative refractory epilepsy. The previous studies have shown the important role of subcortical structures in generation and progression of seizure through cortical subcortical circuits [26,27]. Also a correlation between subcortical gray matter (GM) and age at seizure onset or duration of seizure was also found [28–32].

In this study, ND, ODI, FA and MD images of the patients with MRI-negative refractory epilepsy were first examined visually and then the region of interest (ROI) analysis was performed on cortical regions suspected to be abnormal in the images. Furthermore, because of the importance of cortical-subcortical network interaction in seizure generation, volumes, NODDI and DTI parameters of seven subcortical GM areas (hippocampus, amygdala, thalamus, nucleus accumbens, putamen, caudate and pallidus) of the patients with MRI-negative refractory epilepsy were investigated and compared with the healthy controls. Moreover, the correlations between the volumes, NODDI and DTI parameters of the seven subcortical GM structures and the age at seizure onset and duration of seizure for all the patients with refractory epilepsy were obtained. The main aim of this study was to investigate how ODI, ND, FA and MD will change in cortical and subcortical GMs and whether these changes are correlated with the age at seizure onset and duration of seizure in patients with MRI-negative refractory epilepsy.

2. Methods

2.1. Subjects

At first, 17 patients with MRI-negative refractory epilepsy were selected based on ILAE definition that specified as failure of adequate trials of two tolerated and appropriately chosen anti-epileptic drugs [33]. The participants consisting of four females and 13 males (mean age of 25 years and in the age range of 15 to 45) were scanned with high-resolution MRI scanner. All the patients were intractable to anti-epileptic drug treatments and had MRI-negative scans. The patients were termed “MRI-negative” if two blind radiologists did not recognize any lesion in their routine MRI epilepsy protocols including T1-weighted volumetric acquisition (3D), T1 FLAIR, T2-weighted imaging, T2 FLAIR. The clinical data of the patients have been reported in the Table 1. 19 normal subjects, with no history of neurological and psychiatric disorders were selected as a control group. The mean age of the control group was 29 years (8 females and 11 males in the range of 20–36 years). An approved consent by the Ethical Committee of Tehran University of Medical Sciences was received from each participant.

2.2. MRI acquisition

Images were acquired using a 3.0 T Siemens Magnetom Tim Trio whole body scanner (Siemens AG, Erlangen, Germany), with a 32-channel head coil in patients and controls. Anatomical images were acquired with a high-resolution, T1-weighted MPRAGE (TR = 1800, TE = 3.44 ms, flip angle = 7°, FOV = 256 × 256 mm^2, matrix = 256 × 256 mm^2, voxel size = 1 × 1 × 1 mm). The DWI data were obtained using a single-shot spin echo EPI sequence. Whole-brain diffusion-weighted images were acquired at two different diffusion-weighted sensitizing gradients: b = 700 s/mm^2 with 30 directions and b = 2000 s/mm^2 with 64 directions. The b = 700 s/mm^2 data was used for DTI analysis, while both the b = 700 s/mm^2 and b = 2000 s/mm^2 data were used for the NODDI analysis. The repetition time (TR) and echo time (TE) were 13000 ms and 101 ms for the images acquired at both b = 700 s/mm^2 and b = 2000 s/mm^2, respectively. Additional brain volumes were acquired with no diffusion weighting (b = 0 s/mm^2). The EPI readout uses a matrix size of 128 × 128, FOV of 256 × 256 mm^2, slice thickness of 2 mm and isotropic voxels of 2 × 2 × 2 mm^3. A total of 68 slices were acquired to cover the whole brain. The total acquisition time for diffusion imaging was approximately 30 min.

Table 1
Demographical and clinical characteristic of patients.

Patient	Age (years)	Gender	Age at onset (years)	Duration of seizure (years)	EEG finding
1	20	M	12	8	normal
2	29	M	5	24	Left Occipital
3	45	M	44	1	normal
4	24	M	11	13	Bilateral Frontal
5	15	M	1 month	15	Right Temporal
6	15	M	10	5	Left anterior temporal
7	26	M	3	23	normal
8	25	M	12	13	Left Fronto-Temporal
9	37	M	20	17	Left Fronto-Temporal
10	21	M	19	2	normal
11	40	F	5	35	Bilateral Frontal
12	26	F	5	21	normal
13	15	M	5	10	Left-Frontal
14	25	F	6	19	normal
15	20	F	13	7	Left Temporal
16	15	M	11	4	Right Frontal
17	25	M	10	15	Left Fronto-Central

Gender: F, female; M, male.

2.3. Diffusion image analysis

2.3.1. DTI and NODDI indices calculation

For each subject, all DW scans with b = 700 s/mm^2 were corrected for subject motion and eddy current and EPI distortions with the required B-matrix adjustments. The tensor model was fitted to the corrected data and subsequently, MD and FA were calculated from the tensor's eigenvalues [34]. Data pre-processing was performed using FDT-FSL (FMRIB's Diffusion Toolbox) in multi-shell data. A NODDI microstructural model was computed and fitted to the data using the NODDI Matlab toolbox (http://www.nitrc.org/projects/noddi_toolbox) to generate maps of ND and ODI. In order to limit CSF contamination, a mask containing a CSF fraction below 90% was applied to the ND and ODI maps.

2.4. Manual ROI selection for cortical gray matter

First, we independently assessed ND, ODI, FA and MD maps visually. In region where suspicious lesions were seen on the NODDI maps, their related structural images were re-evaluated by a neuroradiologist. Structural changes were observed in the same areas of the NODDI alterations. Then, ROIs were drawn on observed abnormalities in T1 images by the nueroradiologist. The T1 image was registered to the null image to obtain transformation parameters. The calculated transformation matrix was used to transform the ROI mask to the diffusion space. ROIs were drawn on the lesions and homologous contralateral regions. The mean values and standard deviations in the ROIs were obtained. The contrast-to-noise ratio (CNR) [35] was determined

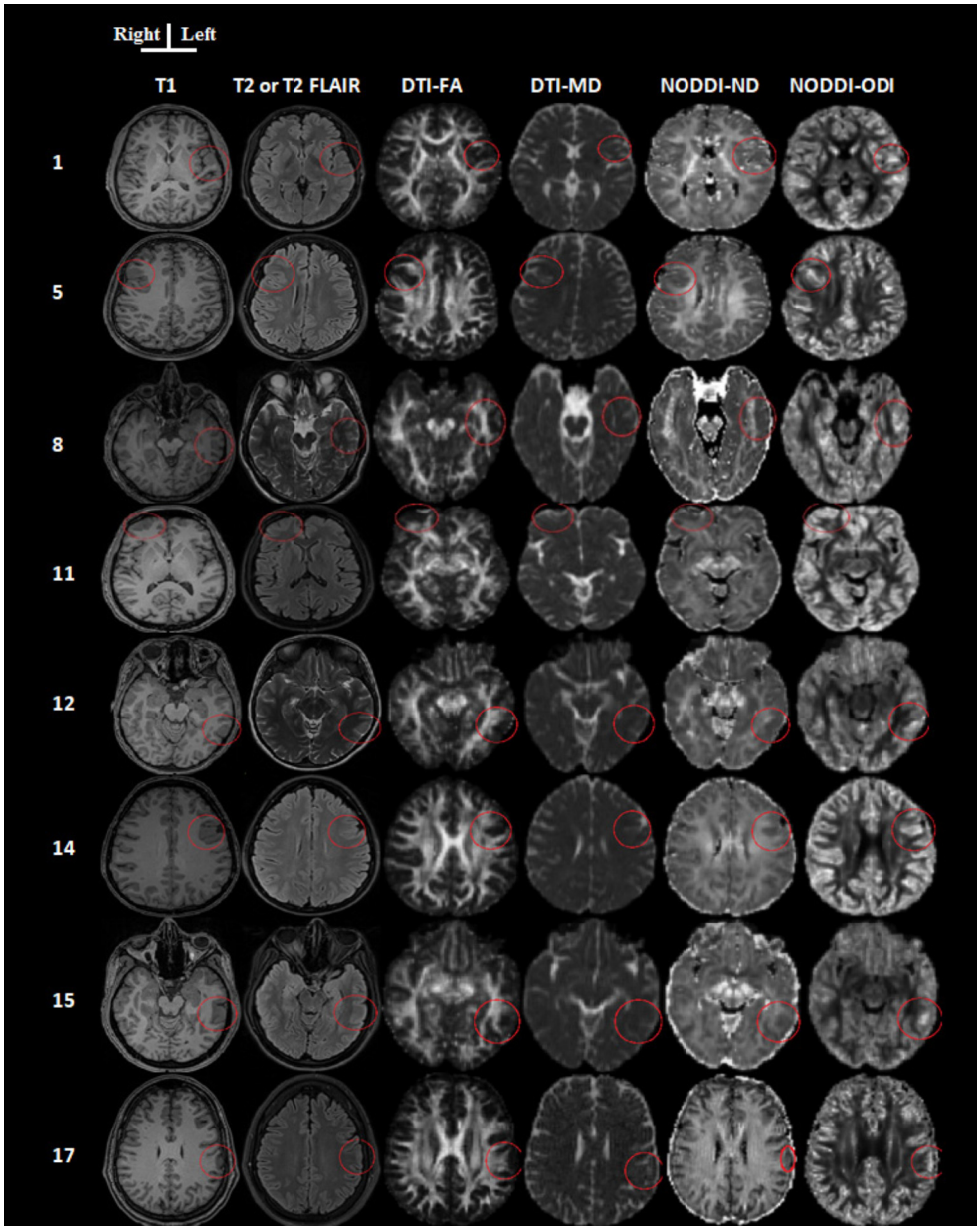

Fig. 1. Structural, NODDI and DTI maps of eight patients with MRI-negative epilepsy.

for the NODDI and DTI maps.

2.5. Subcortical gray matter region selection

Subcortical segmentation were performed on structural 3D T1-weighted images using the FreeSurfer toolkit version 5.3 (http://surfer.nmr.mgh.harvard.edu) to obtain volumetric data and mean values of ND, ODI, FA and MD for seven subcortical GM structures including hippocampus, amygdala, thalamus, accumbens, putamen, caudate and pallidus. The individual T1-weighted MPRAGE images were registered to the null image to obtain transformation parameters. To transform the segmented subcortical mask to the diffusion space the calculated transformation matrix was applied. For each subject, the corresponding volumetric data of the subcortical as well as mean value of ND, ODI, FA and MD were obtained for each segmented subcortical area.

2.6. Statistical analysis

To compare the volumes and the mean values of ND, ODI, FA and MD for the right and left sides of the seven segmented subcortical structures in both of the groups, we first checked the *t*-test assumption of equality of variance and normality in each group. Then, the difference of means in patients and controls were tested by independent two sample *t*-test and the 14 tested ROIs for each parameter and their P-values were reported in Tables S1–S5. The significant difference for each single test was accepted if the uncorrected P-values was less than 0.05.

If we assume that all of the 14 statistical tests conducted in each table are known, then it is possible to calculate the probability of obtaining at least one significant result by chance alone ($1–0.95^{14} = 51\%$). It is also possible to adjust α-levels ($0.05/14 = 0.0035$) for each test to ensure that the probability of making one or several false positives remains at about 5% [36]. Although using such a strict α-threshold is effective in controlling false positive, it inevitably will increase the false negative. If we worried about content of the entire tables to be consistent with the null hypothesis, we can consider the adjustments of α for these large tables containing numerous statistical tests. However, when the results show more than 1

significant effect in each table, suggesting that the results are unlikely to only be false positives. Hence, a threshold of $P < 0.05$ seems fairly reasonable.

To show the strength of difference in patient and control groups in each subcortical, as is well-known, Cohen's d effect sizes were calculated [37]. A larger absolute value of effect size indicates a stronger effect. According to Cohen and Sawilowsky suggestions a value of d greater than 0.8 was considered as a large effect size [37,38]. However, when comparing two groups, a basic issue is specifying whether the groups differ in any manner. To address this issue, we visualized Kernel Density Estimators with Gaussian Kernels of each groups in a plot that is an alternative approach consistent with the graphical perspective of difference [39].

The linear regression analysis was also performed to examine the correlation between the significantly altered volume, DTI and NODDI parameters of subcortical regions and age of seizure onset or duration of seizure. The statistical significance level was considered 0.05.

3. Results

3.1. ROI analysis of cerebral cortical gray matter

ND and ODI images of 17 refractory epilepsy patients with structural MRIs which had been initially interpreted as normal, were assessed visually. Cortical abnormalities as clearly hyperintensity on ODI images were detected for eight patients, qualitatively. Out of these eight patients, in five cases, ND and FA changes were detected as hypointensity and MD changes as hyperintensity in the same area of ODI changes on the cortex. Then ND, ODI, FA and MD images were also examined quantitatively. ROI analysis showed an increase in ODI in abnormal regions relative to homologous regions of the contralateral. The mean of contrast to noise ratio (CNR) of ODI for the eight patients was approximately 1.2 ± 0.58. The mean CNR for ODI was significantly greater than the mean CNR for FA and MD with mean 0.59 ± 0.51 ($p = 0.038$) and mean 0.51 ± 0.18 ($p = 0.029$), respectively. The cortical abnormalities, most likely FCD, were approved in the same areas of ODI changes by a neuroradiologist. Fig. 1 illustrates representative maps of T1 volumetric, T2 or T2 FLAIR, ODI, ND, FA and MD for eight studied patients. NODDI findings, EEG features and seizure semiology of the eight patients and the epilepsy related to their symptoms were reported in the Table 2.

Table 2
Clinical characteristics of eight patients with suspected regions in NODDI and structural imaging.

Patient	NODDI finding	EEG finding	Semiology (signs & symptoms)	Relevant epilepsy
1	Left Frontal	normal	fearing (facially)	Frontal lobe
			dizziness	Temporal lobe
			right hand tonic	Frontal lobe
			loss of consciousness	Temporal lobe
5	Right Frontal	Right Temporal	fearing (facially)	Frontal lobe
			staring	Temporal lobe
			confusion	Frontal and Temporal lobe
			uncontrollable laughing	Frontal and Temporal lobe
			dejavu	Temporal lobe
			loss of consciousness	Temporal lobe
8	Left Temporal	Left Fronto-Temporal	speech arrest	SMA and Temporal lobe
			amnesia	Temporal lobe
			dizziness	Temporal lobe
			confusion	Frontal and Temporal lobe
			loss of consciousness	Temporal lobe
11	Right Frontal	Bilateral Frontal	lip Smacking	Temporal lobe
			screaming	Frontal lobe
			left hand tonic	Frontal lobe
12	Left Temporal	normal	fearing (emotionally)	Temporal lobe
			screaming	Frontal lobe
			amnesia	Temporal lobe
			loss of consciousness	Temporal lobe
14	Left Frontal	normal	fearing (facially)	Frontal lobe
			screaming	Frontal lobe
			loss of consciousness	Temporal lobe
15	Left Temporal	Left Temporal	screaming	Frontal lobe
			lip Smacking	Temporal lobe
			loss of consciousness	Temporal lobe
17	Left Frontal	Left Fronto-central	sudden atonia	Frontal lobe
			vocalization	SMA
			clonic movements	Frontal lobe
			loss of consciousness	Temporal lobe

SMA: supplementary motor area.

3.2. Changes of volumes, DTI and NODDI parameters in subcortical gray matter

The ND values were reduced in the bilateral nucleus accumbens in the patients compared with the controls (Table S1 in Supplementary). The ODI values were increased in the left nucleus accumbens and the right caudate and also reduced in the left amygdala in the patients compared with the controls (Table S2 in Supplementary). The FA values were reduced significantly in the bilateral nucleus accumbens and increased in the bilateral amygdala in the patients groups compared with the controls (Table S3 in Supplementary). The MD values were increased in the left nucleus accumbens, bilateral hippocampus, bilateral putamen, right thalamus and right pallidum in the patients compared with the controls (Table S4 in Supplementary). The volume of right amygdala was increased significantly in patients compared with the controls (Table S5 in Supplementary).

The Chohen's D effect size is also reported in Table S1–S5. The values that are greater than 0.8 are recognizing as 'Large' effect size. To show the strength of difference between patients and control groups, the kernel density estimation of subcorticals with large effect are also visualize in Fig. 2. Therefore, the most important subcorticals to compare the patients and control groups are the ND in the left accumbens and the MD in left putamen, left hippocampus and right pallidum and the FA in left accumbens, the ND in right accumbens, the MD in right putamen and right hippocampus, the FA in the right accumbens, the volume in the right amygdala and the ODI in left accumbens respectively. Fig. 2 illustrates the comparison between the density plots of each group to visualize how these variables identify the patients from the controls.

3.3. Correlation with age at seizure onset and duration of seizure

The age at seizure onset positively correlated with the ODI parameter changes of the left nucleus accumbens ($r = 0.566$, $p = .022$) (Fig. 3A), the right hippocampus ($r = 0.529$, $p = .035$) (Fig. 3B), the left amygdala ($r = 0.553$, $p = .026$) (Fig. 3C) and the left putamen ($r = 0.552$, $p = .027$) (Fig. 3D) also negatively correlated with MD changes of the bilateral nucleus accumbens (regression for right nucleus accumbens: $r = -0.489$, $p = .055$; regression for left nucleus accumbens: $r = -0.6$, $p = .014$) (Fig. 3E). The duration of seizure significantly positively correlated with the mean MD of the right pallidum ($r = 0.502$, $p = .048$) (Fig. 3F).

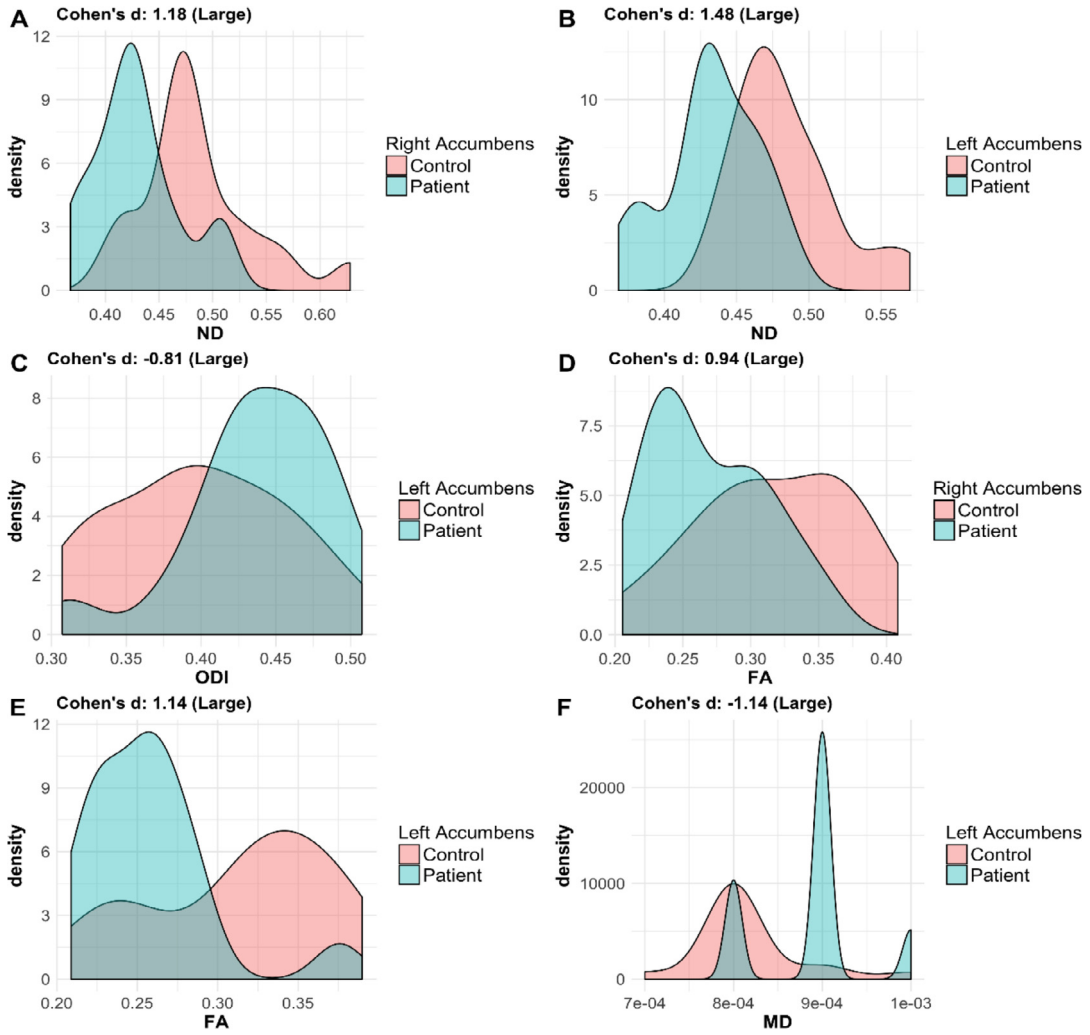

Fig. 2. Empirical density plots for groups of patients and control with (A): ND in right accumbens, (B): ND in left accumbens, (C): ODI in left accumbens, (D): FA in right accumbens, (E): FA in left accumbens, (F): MD in left accumbens, (G): MD in right hippocampus, (H): MD in left hippocampus, (I): MD in right putamen, (J): MD in left putamen, (K): MD in right pallidum and (L): volume in right amygdala. These graphs clearly show the most significant variables for MRI negative epilepsy patients. Since the variance of volume in right amygdala of control cases is greater than patients, the distribution of volume is significantly different in patient and control cases.

4. Discussion

The absence of detectable lesions on the structural MRI is one of the causes of failure in surgical treatment of MRI-negative refractory epilepsy [40]. According to the previous studies, subtle FCD is the most common pathological cause of MRI-negative epilepsy that it is hardly detectable on routine MR imaging techniques [41]. Furthermore, cortical dysplastic areas not limited to one region of the brain [42]. Common MRI features for FCD include cortical thickening, blurring of WM-GM interface and abnormal signal intensity of cortical and subcortical gray matter [43–47]. Previous studies have shown that DTI is a useful method for characterizing abnormalities in patients with MRI negative epilepsy [41,48]. The NODDI as an advanced method in diffusion imaging can separate the various factors in the microstructure changes such as neurite density and fiber orientation dispersion. The NODDI technique is also suitable for both of the WM and GM [24]. Therefore, it is probably more effective in identifying the epileptogenic zone in MRI-negative epilepsy patients with suspected focal cortical dysplasia [49].

In this study, the increased signal intensity in eight patients (out of 17 patients) was clearly visible on ODI images which confirmed by the ROI analysis. By reviewing the routine structural MRI images by a neuroradiologist, all of these abnormal areas were observed as thickening of cortex. Since, cortical thickening is one of the MRI features of FCD, these eight patients can be considered as potential FCD. ND and FA reduction and increase in MD were visually detected in five of these eight patients. The NODDI and structural findings were consistent with the epilepsy related to semiology of the patients. Given that an increase in MD could be due to extracellular space expansion, which can be caused by malformed neurogenesis or cell loss and reduction of FA can be due to decreased neuronal density, increased neuronal dispersion, axonal diameter reduction and demyelination While ND and ODI changes showed reduction of neuronal density and increase of neuronal dispersion, respectively. Therefore, according to the adaptation of the changes in all of these parameters in the five patients, it is suggested that application of NODDI along with DTI can be useful to determine the main cause of these changes.

In this study, there was a significant increase in ODI parameter in comparison with other parameters derived from DTI and NODDI including FA, MD and ND. Winston et al., found a reduction in ND for three patients with FCD and one patient with tuberous sclerosis and reduced ND and increased ODI for one patient with MRI-negative epilepsy [49]. Probably, subtle structural changes can be better identified by ODI parameter rather than DTI and conventional MRI.

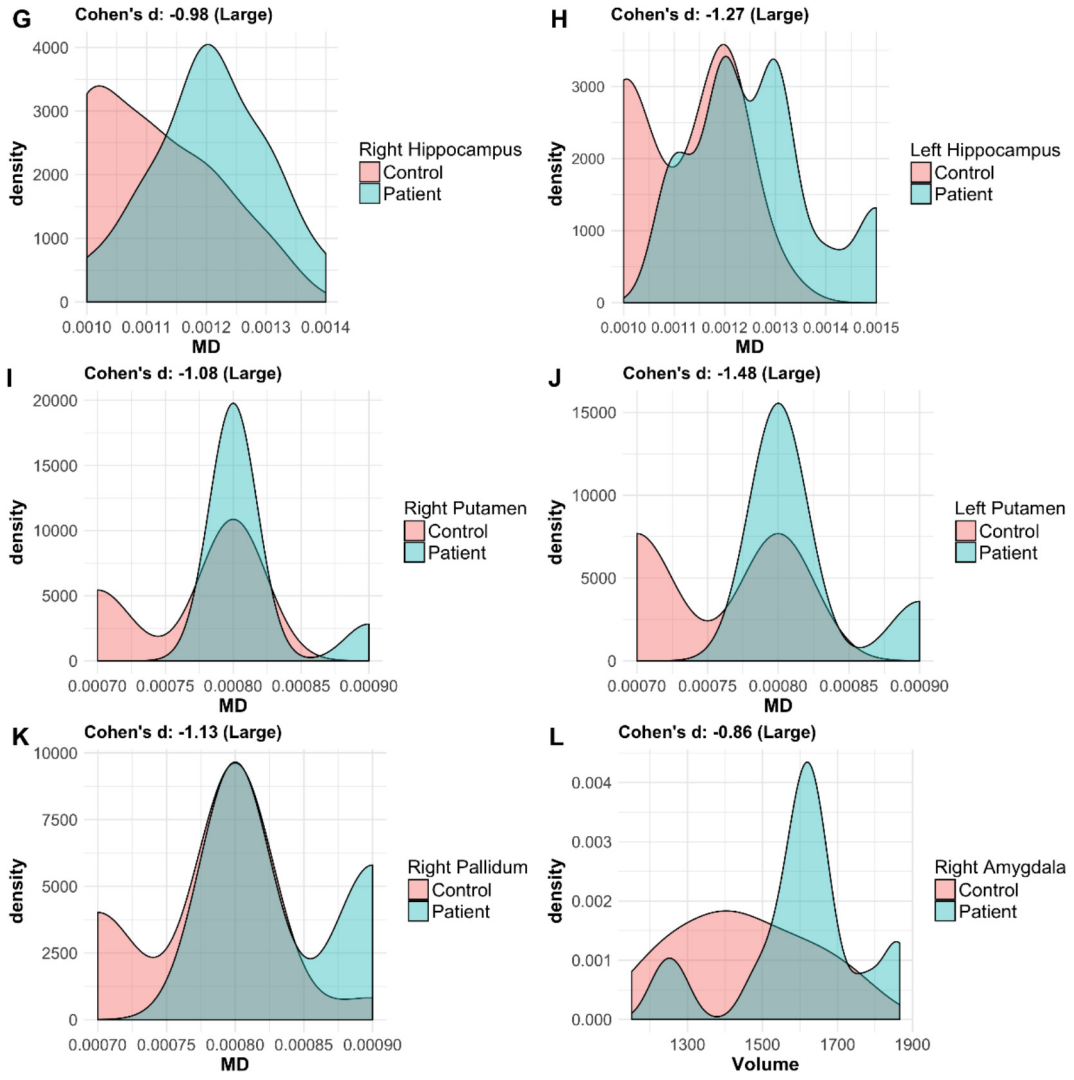

Fig. 2. (*continued*)

The microstructure changes in subcortical gray matter areas can be affected by the chronic period of epilepsy [29,50]. The DTI method is more sensitive than conventional MRI to detect these microstructure changes [29,48]. Microstructure abnormalities of subcortical areas in patients with MRI negative refractory epilepsy have been reported in DTI studies [48]. This study showed a significant increase in the MD parameter in bilateral putamen and right thalamus that was reported in patients with absence epilepsy [29,51] and bilateral hippocampus, right globus pallidus and left nucleus accumbens compared with the control group. Significant FA decreases were found in bilateral nucleus accumbens in patients versus controls. Reduced FA in bilateral nucleus accumbens has been reported by Peng and Harnod for MRI negative cortical epilepsy [48]. Increase of FA was found in bilateral amygdala and the volume of the right amygdala was also increased significantly in the patients compared with the controls. This increase in amygdala volume is consistent with the study of Singh and Kaur in temporal lobe epilepsy patients with normal MRI [52].

It is founded that age at seizure onset was significantly negatively correlated with the mean MD of bilateral nucleus accumbens as well as duration of seizure positively correlated with the mean MD of right pallidum. According to the results of biological studies, ND and ODI in the NODDI have a higher sensitivity to the FA and are more specific to show abnormal areas [53]. Therefore, in this study, NODDI was applied for subcortical GM microstructural and its correlation with age at seizure onset and progression of the diseases. NODDI analysis revealed that ODI was reduced in left amygdala and increased in left nucleus accumbens and right caudate and reduction of ND was also detected in bilateral nucleus accumbens. The results showed decrease of ODI and increase of FA in the left amygdala, as ODI correlates with FA inversely [53]. Although the *t*-test analysis was significant for some of the parameters, the comparison of densities showed that distribution of patients and controls were not different significantly. Comparison of the density plots in each group showed how these variables separate the patients from the controls. The results of Cohen's d effect sizes represented that the parameters with d greater than 0.8 are the most important variables and should be inspected in more details in patients with MRI-negative refractory epilepsy.

There was a significant positive correlation between age at seizure onset and the mean ODI of left accumbens, left amygdala, left putamen and right hippocampus that has not yet been reported. This relationship supports the hypothesis that ODI alterations of the subcortical gray matter are related to epilepsy progression such as relationships of FA and MD with age at seizure onset and duration of epilepsy [54].

5. Conclusions

The results of this study revealed that advances in DTI techniques will help improve the understanding of subtle structural abnormalities in cortical, subcortical gray matter changes and progression of epilepsy in MRI negative refractory patients. However, a post-surgical histology

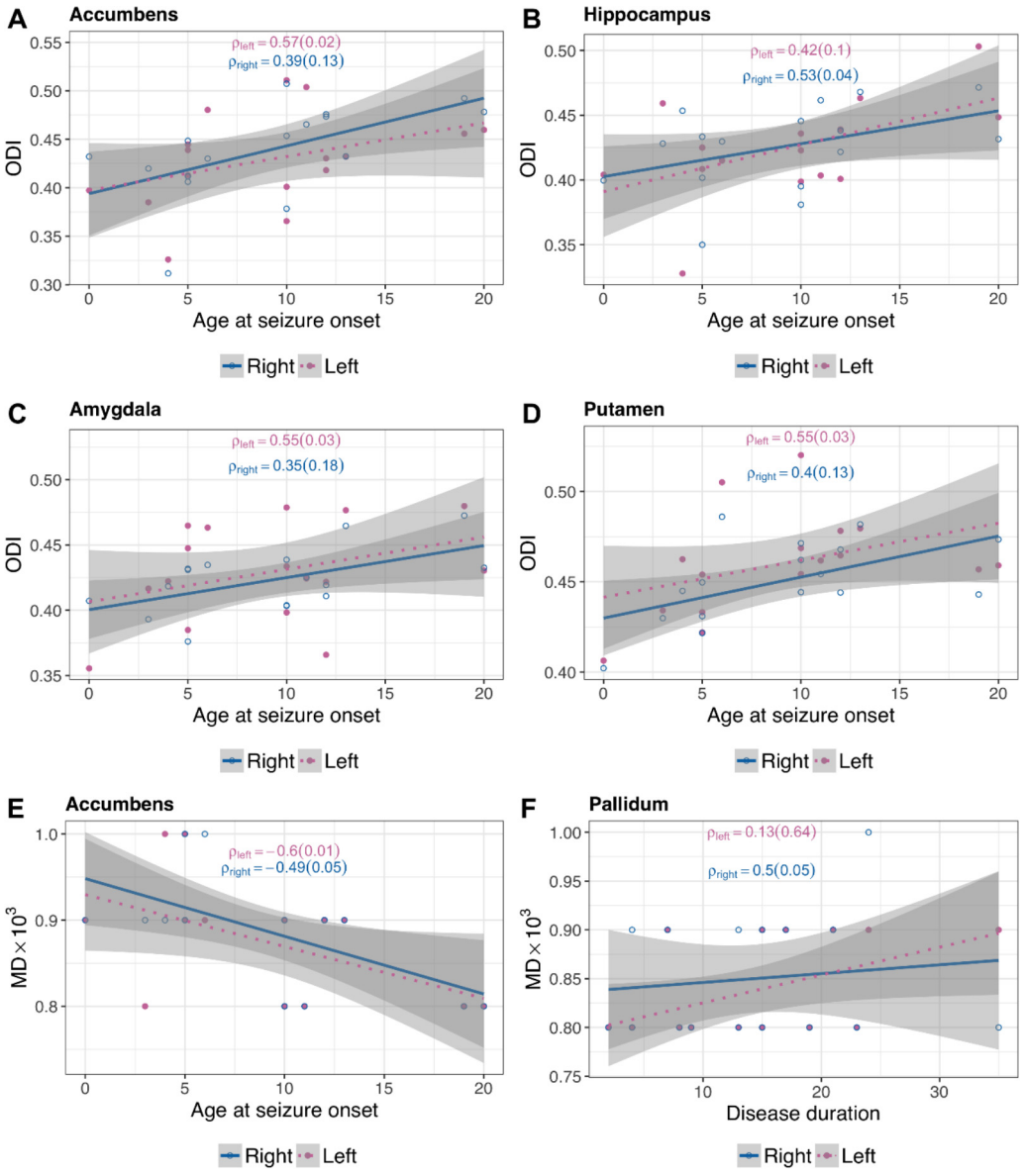

Fig. 3. The scatterplots of the significant relationship of subcorticals with age at seizure onset and disease duration. (A) The accumbens measured with ODI (B) the hippocampus measured with ODI (C) the amygdala measured with ODI (D) the putamen measured with ODI (E) the accumbens measured with MD (F) the pallidum measured with MD.

study is required to confirm microstructural changes in cortical and subcortical gray matter.

Acknowledgement

The authors are grateful to the Vice Chancellor for Research and Technology, Tehran University of Medical Sciences Grant (94-02-30-28454) for supporting this project.

Appendix A. Supplementary data

Supplementary data associated with this article can be found, in the online version, at http://dx.doi.org/10.1016/j.ejmp.2018.03.005.

References

[1] Fisher R, Stein A, Karis J. Epilepsy for the neuroradiologist. AJNR Am J Neuroradiol 1997;18(5):851–63.
[2] Rastogi S, Lee C, Salamon N. Neuroimaging in pediatric epilepsy: a multimodality approach 1. Radiographics 2008;28(4):1079–95.
[3] Snead OC. Surgical treatment of medically refractory epilepsy in childhood. Brain Dev 2001;23(4):199–207.
[4] Kwan P, Brodie MJ. Early identification of refractory epilepsy. N Engl J Med 2000;342(5):314–9.
[5] Engel Jr J. Surgery for seizures. N Engl J Med 1996;334(10):647–53.
[6] Siegel AM, Jobst BC, Thadani VM, Rhodes CH, Lewis PJ, Roberts DW, et al. Medically intractable, localization-related epilepsy with normal MRI: presurgical evaluation and surgical outcome in 43 patients. Epilepsia 2001;42(7):883–8.
[7] Téllez-Zenteno JF, Dhar R, Wiebe S. Long-term seizure outcomes following epilepsy surgery: a systematic review and meta-analysis. Brain 2005;128(5):1188–98.
[8] Berkovic SF, McIntosh A, Kalnins RM, Jackson GD, Fabinyi G, Brazenor G, et al. Preoperative MRI predicts outcome of temporal lobectomy an actuarial analysis. Neurology 1995;45(7):1358–63.
[9] Duncan JS. Imaging and epilepsy. Brain 1997;120(2):339–77.
[10] Carne R, O'Brien T, Kilpatrick C, MacGregor L, Hicks R, Murphy M, et al. MRI-negative PET-positive temporal lobe epilepsy: a distinct surgically remediable syndrome. Brain 2004;127(10):2276–85.
[11] Hong K-S, Lee SK, Kim J-Y, Lee D-S, Chung C-K. Pre-surgical evaluation and surgical outcome of 41 patients with non-lesional neocortical epilepsy. Seizure 2002;11(3):184–92.
[12] Kutsy RL. Focal extratemporal epilepsy: clinical features, EEG patterns, and surgical approach. J Neurol Sci 1999;166(1):1–15.
[13] Wang ZI, Alexopoulos AV, Jones SE, Jaisani Z, Najm IM, Prayson RA. The pathology

of magnetic-resonance-imaging-negative epilepsy. Mod Pathol 2013;26(8):1051–8.
[14] Krsek P, Hajek M, Dezortova M, Jiru F, Skoch A, Marusic P, et al. 1H MR spectroscopic imaging in patients with MRI-negative extratemporal epilepsy: correlation with ictal onset zone and histopathology. Eur Radiol 2007;17(8):2126–35.
[15] McGonigal A, Bartolomei F, Régis J, Guye M, Gavaret M, Fonseca AT-D, et al. Stereoelectroencephalography in presurgical assessment of MRI-negative epilepsy. Brain 2007;130(12):3169–83.
[16] Jeha LE, Najm I, Bingaman W, Dinner D, Widdess-Walsh P, Lüders H. Surgical outcome and prognostic factors of frontal lobe epilepsy surgery. Brain 2007;130(2):574–84.
[17] Lee SK, Lee SY, Kim KK, Hong KS, Lee DS, Chung CK. Surgical outcome and prognostic factors of cryptogenic neocortical epilepsy. Ann Neurol 2005;58(4):525–32.
[18] Nobili L, Francione S, Mai R, Cardinale F, Castana L, Tassi L, et al. Surgical treatment of drug-resistant nocturnal frontal lobe epilepsy. Brain 2007;130(2):561–73.
[19] Bien CG, Szinay M, Wagner J, Clusmann H, Becker AJ, Urbach H. Characteristics and surgical outcomes of patients with refractory magnetic resonance imaging–negative epilepsies. Arch Neurol 2009;66(12):1491–9.
[20] Bast T. Outcome after epilepsy surgery in children with MRI-negative non-idiopathic focal epilepsies. Epileptic Disord 2013;15(2):105–13.
[21] Thivard L, Adam C, Hasboun D, Clémenceau S, Dezamis E, Lehéricy S, et al. Interictal diffusion MRI in partial epilepsies explored with intracerebral electrodes. Brain 2006;129(2):375–85.
[22] Rugg-Gunn F, Eriksson S, Symms M, Barker G, Duncan J. Diffusion tensor imaging of cryptogenic and acquired partial epilepsies. Brain 2001;124(3):627–36.
[23] Chen Q, Lui S, Li C-X, Jiang L-J, Ou-Yang L, Tang H-H, et al. MRI-negative refractory partial epilepsy: role for diffusion tensor imaging in high field MRI. Epilepsy Res 2008;80(1):83–9.
[24] Zhang H, Schneider T, Wheeler-Kingshott CA, Alexander DC. NODDI: practical in vivo neurite orientation dispersion and density imaging of the human brain. Neuroimage 2012;61(4):1000–16.
[25] Chung AW, Seunarine KK, Clark CA. NODDI reproducibility and variability with magnetic field strength: a comparison between 1.5 T and 3 T. Hum Brain Mapp 2016;37(12):4550–65.
[26] Bertram EH. Neuronal circuits in epilepsy: do they matter? Exp Neurol 2013;244:67–74.
[27] Berman R, Negishi M, Vestal M, Spann M, Chung MH, Bai X, et al. Simultaneous EEG, fMRI, and behavior in typical childhood absence seizures. Epilepsia 2010;51(10):2011–22.
[28] Saini J, Sinha S, Bagepally B, Ramchandraiah C, Thennarasu K, Prasad C, et al. Subcortical structural abnormalities in juvenile myoclonic epilepsy (JME): MR volumetry and vertex based analysis. Seizure 2013;22(3):230–5.
[29] Luo C, Xia Y, Li Q, Xue K, Lai Y, Gong Q, et al. Diffusion and volumetry abnormalities in subcortical nuclei of patients with absence seizures. Epilepsia 2011;52(6):1092–9.
[30] Keller SS, Ahrens T, Mohammadi S, Möddel G, Kugel H, Bernd Ringelstein E, et al. Microstructural and volumetric abnormalities of the putamen in juvenile myoclonic epilepsy. Epilepsia 2011;52(9):1715–24.
[31] Szabo C, Lancaster J, Lee S, Xiong J-H, Cook C, Mayes B, et al. MR imaging volumetry of subcortical structures and cerebellar hemispheres in temporal lobe epilepsy. AJNR Am J Neuroradiol 2006;27(10):2155–60.
[32] Dreifuss S, Vingerhoets F, Lazeyras F, Andino SG, Spinelli L, Delavelle J, et al. Volumetric measurements of subcortical nuclei in patients with temporal lobe epilepsy. Neurology 2001;57(9):1636–41.
[33] Kwan P, Arzimanoglou A, Berg AT, Brodie MJ, Allen Hauser W, Mathern G, et al. Definition of drug resistant epilepsy: consensus proposal by the ad hoc Task Force of the ILAE Commission on Therapeutic Strategies. Epilepsia 2010;51(6):1069–77.
[34] Leemans A, Jeurissen B, Sijbers J, Jones D, editors. ExploreDTI: a graphical toolbox for processing, analyzing, and visualizing diffusion MR data. In: 17th Annual Meeting of Intl Soc Mag Reson Med; 2009.
[35] Song X, Pogue BW, Jiang S, Doyley MM, Dehghani H, Tosteson TD, et al. Automated region detection based on the contrast-to-noise ratio in near-infrared tomography. Appl Opt 2004;43(5):1053–62.
[36] Dunn OJ. Multiple comparisons among means. J Am Stat Assoc 1961;56(293):52–64.
[37] Cohen J. Statistical power analysis for the behavioral sciences. NY, New York: Routledge; 1988.
[38] Sawilowsky SS. New effect size rules of thumb; 2009.
[39] Wilcox RR. Kernel density estimators: an approach to understanding how groups differ. Understand Stat 2004;3(4):333–48.
[40] Téllez-Zenteno JF, Ronquillo LH, Moien-Afshari F, Wiebe S. Surgical outcomes in lesional and non-lesional epilepsy: a systematic review and meta-analysis. Epilepsy Res 2010;89(2):310–8.
[41] Widjaja E, Geibprasert S, Otsubo H, Snead O, Mahmoodabadi S. Diffusion tensor imaging assessment of the epileptogenic zone in children with localization-related epilepsy. AJNR Am J Neuroradiol 2011;32(10):1789–94.
[42] Fauser S, Sisodiya SM, Martinian L, Thom M, Gumbinger C, Huppertz H-J, et al. Multi-focal occurrence of cortical dysplasia in epilepsy patients. Brain 2009;132(8):2079–90.
[43] Kuzniecky RI, Barkovich AJ. Malformations of cortical development and epilepsy. Brain Dev 2001;23(1):2–11.
[44] Colombo N, Tassi L, Galli C, Citterio A, Russo GL, Scialfa G, et al. Focal cortical dysplasias: MR imaging, histopathologic, and clinical correlations in surgically treated patients with epilepsy. AJNR Am J Neuroradiol 2003;24(4):724–33.
[45] Seifer G, Blenkmann A, Princich JP, Consalvo D, Papayannis C, Muravchik C, et al. Noninvasive approach to focal cortical dysplasias: clinical, EEG, and neuroimaging features. Epilepsy Res Treat 2012;2012.
[46] Barkovich AJ, Kuzniecky RI. Neuroimaging of focal malformations of cortical development. J Clin Neurophysiol 1996;13(6):481–94.
[47] Barkovich AJ, Kuzniecky RI, Bollen AW, Grant PE. Focal transmantle dysplasia: a specific malformation of cortical development. Neurology 1997;49(4):1148–52.
[48] Peng S-J, Harnod T, Tsai J-Z, Ker M-D, Chiou J-C, Chiueh H, et al. Evaluation of subcortical grey matter abnormalities in patients with MRI-negative cortical epilepsy determined through structural and tensor magnetic resonance imaging. BMC Neurol 2014;14(1):1.
[49] Winston GP, Micallef C, Symms MR, Alexander DC, Duncan JS, Zhang H. Advanced diffusion imaging sequences could aid assessing patients with focal cortical dysplasia and epilepsy. Epilepsy Res 2014;108(2):336–9.
[50] Liu Z, Xu Y, An J, Wang J, Yin X, Huang R, et al. Altered brain white matter integrity in temporal lobe epilepsy: a TBSS study. J Neuroimaging 2015;25(3):460–4.
[51] Yang T, Guo Z, Luo C, Li Q, Yan B, Liu L, et al. White matter impairment in the basal ganglia-thalamocortical circuit of drug-naive childhood absence epilepsy. Epilepsy Res 2012;99(3):267–73.
[52] Singh P, Kaur R, Saggar K, Singh G, Aggarwal S. Amygdala volumetry in patients with temporal lobe epilepsy and normal magnetic resonance imaging. Pol J Radiol 2016;81:212.
[53] Timmers I, Roebroeck A, Bastiani M, Jansma B, Rubio-Gozalbo E, Zhang H. Assessing microstructural substrates of white matter abnormalities: a comparative study using DTI and NODDI. PLoS One 2016;11(12):e0167884.
[54] Keller SS, Schoene-Bake J-C, Gerdes JS, Weber B, Deppe M. Concomitant fractional anisotropy and volumetric abnormalities in temporal lobe epilepsy: cross-sectional evidence for progressive neurologic injury. PLoS One 2012;7(10):e46791.